Seasonal heterogeneity in the impact of air exposure on the photophysiology of two tropical intertidal seagrass species (*Zostera muelleri* ssp. *capricorni* and *Halophila ovalis*)

K. Petrou[1*], I. Jimenez-Denness[1], K. Chartrand[2], C. McCormack[2], M. Rasheed[2] and P. J. Ralph[1]

[1]Plant Functional Biology and Climate Change Cluster and School of Environment, University of Technology, Sydney, PO Box 123, Broadway, New South Wales, 2007, Australia.

[2] Marine Ecology Group, Northern Fisheries Centre, Fisheries Queensland, Department of Agriculture, Fisheries and Forestry, PO Box 5396, Cairns, Queensland 4870, Australia.

[*]Corresponding author:
Katherina Petrou email: katherina.petrou@uts.edu.au

Running head: Tidal effects on seagrass photosynthesis

Abstract

Photosynthesis, chlorophyll *a* fluorescence, leaf bio-optical properties and pigments were measured in two tropical intertidal seagrass species, *Zostera muelleri* ssp. *capricorni* and *Halophila ovalis* before, during and after air-exposure over a tidal cycle. Data were collected across four seasons (October and January – growing season; May and July – senescent season) to determine seasonal dynamics in physiological responses to air exposure. Both species showed clear light-dependent responses with a decline in photosynthetic efficiency and increased photoprotection during periods of combined maximum daily irradiance and air exposure for all seasons. In *Z. muelleri* ssp. *capricorni* there was a negative correlation between air exposed effective quantum yield and light intensity, suggesting exposure was driving this decline. Conversely, sensitivity (decline in effective quantum yield of photosystem II) to increased irradiance dominated the response in *H. ovalis*, with no change in the magnitude of this response between air-exposed and submerged blades. The response to air exposure observed in *Z. muelleri* ssp. *capricorni* showed seasonal variation, with a greater decline in photosynthesis during the spring. Tidal exposure did not provide intertidal seagrasses a 'window' of photosynthetic respite (increase in photosynthesis) from high natural or anthropogenic related turbidity. However, the periods immediately prior to and after exposure were important for providing an optimum period for net photosynthetic gain.

Keywords: Seagrass, chlorophyll *a* fluorescence, light-limitation, air exposure.

Introduction

Seagrass meadows are highly productive coastal habitats, important in nutrient cycling, carbon sequestering and supporting commercially valuable fisheries through the provision of

habitat and food (Orth et al. 2006, Rasheed et al. 2008, Unsworth and Cullen 2010). Globally, seagrass meadows occupy the coastal regions of tropical and temperate waters. Productivity of seagrasses, as with all plants, is driven by photosynthesis, which in turn is regulated by light, temperature and nutrient availability. In general, the minimum light requirement to maintain seagrass health (growth and photosynthesis) is relatively high (Duarte 1991, Dennison et al 1993); however tolerance to light deprivation often varies among species (Longstaff and Dennison 1999).

Seagrass meadows that grow in the intertidal zone are exposed to highly variable and often extreme environmental conditions (Rasheed and Unsworth 2011; Taylor and Rasheed 2012). Tidal oscillations that change asynchronously with diurnal irradiance mean that seagrasses are subject to large fluctuations in temperature and light. At times where the maximum irradiance and midday (air and water) temperature maximum coincide with low tide, intertidal seagrasses are vulnerable to thermal stress, desiccation and possible photosynthetic damage as a result of persistent photoinhibitory irradiances. Seagrasses need to constantly balance their use of captured photons for photosynthesis and the need for photoprotection from excess irradiance and other photosynthetic stress factors. This balance is achieved by adjusting their photosynthetic activity and pigments in response to light (Ralph 1998).

Light is considered the most important determinant of seagrass productivity, distribution and abundance (Dennison et al 1993, Abal and Dennison 1996). In many coastal habitats, light quantity and quality may change rapidly with increased light scattering and attenuation due to suspended particles greatly altering light availability for seagrasses (Zimmerman et al. 1991, Longstaff and Dennison 1999). Increased turbidity can result from natural processes such as storm events and tidal flux or catchment runoff after high rainfall. Additionally, it can be the result of anthropogenic activities such as poor land management practices leading to

increased sediment loads in the coastal zone or port and dredge operations that re-suspend sediments, both causing significant light attenuation (Ralph et al 2007).

Along the Queensland coast, many estuaries are naturally subject to large tidal fluxes and an associated constant re-suspension of sediment, creating a highly turbid light environment for intertidal seagrasses. Shallow seagrass meadows often become air-exposed during the day, altering photosynthetic condition and potentially affecting oxygen production (Johnston and Raven 1986). Exposure or near exposure at the lower tidal range may actually provide short periods of time for an increase in photosynthesis due to the increase in available light or as a result of increased CO_2 assimilation rates, due to the decreased resistance for CO_2 diffusion (Johnston and Raven 1986, Beer and Rehnberg 1997). In highly turbid conditions where plants are light-limited, periods of high light, while still submerged or air-exposed, may provide a "window" of photosynthetic relief from high turbidity during low tide. Alternatively, if irradiances become too high or desiccation too prolonged during these periods it could lead to severe light stress on photosynthetic tissues and even damage the photosystems (Seddon and Cheshire 2001). It is also possible that exposed seagrass blades exceed their thermal tolerance for photosynthesis when exposed for long periods at low tide which would also lead to a decline in net photosynthesis (Leuschner et al. 1998). Given the complex growing conditions that intertidal seagrasses are exposed to, it is necessary to understand how photosynthesis is impacted by the daily tidal cycle and periodic air exposure. In this study, we aim to determine whether this 'window' of exposure during a tidal cycle actually results in an increase in photosynthesis for these intertidal seagrasses living in turbid environments.

Here we investigate the effect of tidal flux on the photochemical efficiency, photoprotective pigment ratios and oxygen production of intertidal seagrass meadows from Gladstone

Harbour over a tidal cycle across different seasons. Specifically, this study aims to measure changes in photosynthesis during exposure events, to better understand how exposure and near-exposure (shallow water) influences seagrass physiology and production. This study focuses on two seagrass species whose distributions overlap on Australia's northeast coast; *Halophila ovalis* (R. Br.) Hook. *f.*, a widespread tropical species and *Zostera muelleri* ssp. *capricorni* (Ascherson), a species endemic to Australia that occurs only in shallow coastal tropical and sub-tropical waters. While this study is limited in its ability to provide significant causality to changes in photosynthesis upon exposure, the quarterly sampling does provide some understanding of the variability in the responses to air exposure in seagrasses over an annual cycle and helps to differentiate possible effects of temperature stress, with lower water temperatures in the senescent season compared with the growing season.

Materials and Methods

Study site and sampling protocol

The study site was an intertidal seagrass meadow at Pelican Banks, Gladstone Harbour (151.308456; -23.766299) where two intertidal seagrass species *Zostera muelleri* ssp. *capricorni* and *Halophila ovalis* form the dominant benthic habitat. The seagrass meadows of Pelican Banks are subject to a semi-diurnal tidal cycle with two high and two low tides each day and an average spring tidal range of about 5 m. Due to the tidal activity, the site is fairly turbid, particularly on the extreme of each incoming and outgoing tide. The maximum Nephelometric Turbidity Units (NTU) during the study months were 321.9 (October), 61.8 (January), 48.7 (May) and 21.45 (July) (data sourced from Vision Environment, QLD). Field measurements were made over one or two days on four separate field trips, each during different seasons –spring (22nd and 24th October, 2010), summer (19th and 20th January,

2011), autumn (14th May, 2011) and winter (14th July, 2011). Mean water temperatures for the months sampled were 23.69 ± 1.14 (Oct), 27.25 ± 0.67 (Jan), 21.45 ± 1.52 (May) and 18.18 ± 0.59ºC (July), while mean monthly solar irradiances were 12.30 ± 7.12, 6.56 ± 2.56, 5.76 ± 3.50 and 14.28 ± 4.06 mol photons m^{-2} d^{-1} for the same months, respectively. Physiological measurements were made from before solar noon until sundown at near-hourly intervals starting three hours prior to the absolute low tide. This sampling protocol was used to ensure that before, during and after air exposure photosynthetic activity was captured in the sampling program. Chlorophyll *a* fluorescence measurements were performed using SCUBA divers to capture *in situ* photosynthetic activity and leaf samples (2nd blade) were collected by the divers and measurements including oxygen production and bio-optical properties were taken on board the vessel. Leaf blades were also collected and immediately frozen in liquid nitrogen for later HPLC pigment determinations of the state of the xanthophyll cycle.

Chlorophyll a fluorescence

Chlorophyll *a* fluorescence measurements were performed using a Pulse Amplitude Modulated fluorometer (Diving-PAM; Walz GmbH, Effeltrich, Germany). Rapid light curves (RLCs) were measured on leaf blades using the in-built software routine of nine incrementing actinic illumination steps (0, 33, 72, 117, 178, 249, 375, 512, 780 µmol photons m^{-2} s^{-1}) at 10 s intervals. A specialised leaf clip was used to position the fibre optic probe at a fixed distance from the leaf blade for each measurement. All measurements were performed on the second leaf blade to be comparable across all plants. Six independent leaf blades were measured every 1–2 h on the outgoing and incoming tides, before during and, where possible, after air exposure.

Relative electron transport rate (rETR) was calculated as the product of effective quantum yield (Φ_{PSII}) and irradiance (µmol photons m^{-2} s^{-1}). Data were fitted according to the double exponential function as in Ralph and Gademann (2005) and three photosynthetic parameters; maximum electron transport rate ($rETR_{max}$), light utilisation efficiency (α) and minimum saturating irradiance (E_k) were derived from these curves. Initial effective quantum yield of PSII (Yi) taken as the first Φ_{PSII} value (Φ_{PSII} at *in situ* irradiance) from each RLC was plotted as a function of irradiance for both *Halophila ovalis* and *Zostera muelleri* ssp. *capricorni* to help differentiate a light-dependent from an exposure-dependent response and a linear regression analysis was applied to the data.

Direct O_2 measurements

Rates of photosynthesis were determined before, during and after exposure at low tide by measuring oxygen (O_2) evolution inside 5 ml air- and water-tight incubation bottles equipped with oxygen sensitive luminescent material and read by an optical sensor (SDR SensorDish Reader, Presens, Germany). Leaves (2^{nd} blade) were collected at 1-2 h intervals between 10:00 and 17:00 h on each of the sampling days and processed on board within 1-2 h. Leaves were cleaned of epiphytes and placed into the incubation bottles filled with filtered (pore size 0.2 µm) seawater (3 to 5 leaves per bottle, *n*= 6 bottles). Oxygen concentrations within each bottle were measured at the start (t0) and end (t1) of a 20 min dark incubation period within a constant temperature seawater bath (same as the *in situ* temperature). After respiration measurements (R_D), the bottles were then placed into a transparent chamber that was returned to the seabed for 30 min of *in situ* light incubation, and recovered for measurement of the final O_2 concentration (t2). Rates of gross oxygenic production (P_G) within each bottle were determined as: $P_G = P_N - R_D$, where P_N and R_D are the net photosynthesis measured in the

light and the respiration in the dark, respectively. Productivity was normalized to total leaf area in the bottle and reported as µmol O_2 cm^{-2} h^{-1}.

Leaf-specific absorptance A(λ)

Leaf-specific absorptance is a measure of the fraction of photosynthetically active radiation (PAR) captured by the leaf's photosynthetic pigments. Leaf spectral transmittance and reflectance were measured from 400 to 750 nm at 1 nm resolution using two fibre optic spectrometers (USB2000+ and USB2000 Ocean Optics, USA) interfaced with two integrating spheres (FOIS-1 and ISP-REF, Ocean Optics, USA). Leaves collected from the seagrass meadow were placed in numbered plastic containers and kept moist and in the dark until optical properties were measured (within ~1 hour). Leaves were gently scraped clean of epiphytes and placed between two microscope slides. Black tape was used to obscure the portion of the sample port not covered by leaf tissue.

For transmittance measurements, a tungsten halogen light source (LS-1, Ocean Optics, USA) was adjusted to completely irradiate the 9.5 mm diameter sample port of the integrating sphere (FOIS-1, Ocean Optics, USA). Leaf spectral transmittance (T(λ)) was calculated with reference to the slide and tape without a leaf in place. For reflectance measurements, the sample was placed over the port of the second integrating sphere (ISP-Ocean Optics, USA) so that the same side faced the light source (internal to the sphere in the case of the ISP-Ocean Optics). Leaf spectral reflectance (R(λ)) was calculated, referenced to the slide and tape with a diffusive reflectance standard (Spectralon 98%). Leaf-specific absorptance A(λ) was then calculated as:

$$A(\lambda) = 1 - T(\lambda) - R(\lambda) - A(750\ nm)$$

187 Where A(750 nm) is a correction for non-photosynthetic absorptance:

188 $$A(750\ nm) = 1 - T(750\ nm) - R(750\ nm)$$

189 Leaf-specific photosynthetic absorptance AΦ (PAR) was calculated as the spectral average of
190 A(λ) over the spectral range 400-700 nm (Durako 2007).

191

192 *Leaf optical cross section a*(λ)*

193 Leaf optical cross section (*a**) is a measure of chlorophyll use efficiency. The collected
194 leaves were photographed and their surface area was determined digitally using image
195 analysis software (ImageJ). Pigments were then extracted by grinding weighed leaf samples
196 in ice cold 80% acetone using a mortar and pestle with clean sand. Concentrations of
197 chlorophyll *a* (Chl *a*) and *b* (Chl *b*) were determined spectrophotometrically using the
198 equations and extinction coefficients of Jeffrey and Humphrey (1975). The leaf-specific
199 absorption coefficient a(λ) was calculated from the absorptance A(λ) as -ln [1-A(λ)] and the
200 optical cross-section a*(λ) was calculated by normalizing a(λ) to the area specific Chl *a*
201 concentration (Enríquez 2005):

202 $$a^*(\lambda) = a(\lambda) / [\text{Chl } a]$$

203

204 *Photoprotective pigments*

205 Pigment concentrations were determined using high performance liquid chromatography
206 (HPLC). Pigments were extracted by grinding and analysed according to the methods of van
207 Heukelem and Thomas (2001) with the only modification being an extra filtration step
208 through 0.2 µm PTFE 13 mm syringe filters (Micro-Analytix Pty Ltd). Clarified samples

were stored in amber HPLC glass vials (Waters Australia Pty Ltd, Australia) at -80 °C overnight before analysis. The HPLC system included a pump, temperature-controlled auto-injector (Waters Australia Pty Ltd, Australia), C8 column (150 x 4.6 mm; Eclipse XDB), and photodiode array detector (Waters Australia Pty Ltd, Australia). Pigments were identified by comparison of their retention times and spectra using calibration standards (DHI, Denmark) for each pigment. Peaks were integrated using curve-fitting software (Empower Pro Waters Australia Pty Ltd, Australia) and checked manually to confirm the accuracy of the peak baselines and the similarity of the integrated peaks to that of the standard. The pigment data were used to investigate rapid photoprotective responses over a tidal cycle by measuring the de-epoxidation state of violaxanthin (a measure of violaxanthin conversion to the photoprotective zeaxanthin). This was calculated as: ((Zeaxanthin) + (0.5*Antheraxanthin)) / (Violaxanthin + Antheraxanthin + Zeaxanthin) (Thayer and Björkman 1990).

Underwater light climate

Down-welling photosynthetically active radiation (PAR) at the water surface and seafloor were measured at each sampling period using a 2Π underwater quantum sensor (LI192SA, LI-COR Nebraska, USA) attached to a frame and a photometer (LI-1400, LI-COR Nebraska, USA). Water depth was also measured at each time point of sampling.

Data analysis

To test for significant differences in the photosynthetic parameters and oxygen production throughout the tidal cycle a one-way analysis of variance (ANOVA) was used at $\alpha = 0.05$ and pairwise comparisons made using a Tukey's post hoc test. To ensure that the assumption of

equal variances for all parametric tests was satisfied, a Levene's test for homogeneity of variance was applied to all data *a priori*. In cases where the assumption of homoscedasticity was not met, data were log transformed before analysis or a non-parametric Kruskal-Wallis test was used instead. All analyses were performed using Minitab statistical software (version 15.1.0.0 2006, Pennsylvania, USA).

Results

Spring (growing season)

Maximum daily irradiance coincided with the time just prior to air exposure on both sampling days, but stayed around the same intensity (543-733 µmol photons m^{-2} s^{-1}) during the exposure event (Fig. 1a and b). Due to the nature of the measurements, oxygen data could only be measured in water (as the instrument relies on aqueous phase). Therefore, samples were taken immediately prior to exposure and after 1 h of complete air exposure. Oxygen production showed a significant decrease after exposure in *Zostera muelleri* ssp. *capricorni* ($P < 0.05$; Fig 1c). The same response was measured in *Halophila ovalis*, whereby O_2 production following air exposure was significantly lower than during the immersed periods ($P < 0.05$; Fig 1d). Seagrass photosynthetic light absorption capacity remained constant for *Z. muelleri* ssp. *capricorni* and *H. ovalis* (0.62 ± 0.12, 0.46 ± 0.09, respectively) throughout the tidal exposure event. The photoprotective pigment ratios determined by HPLC analysis showed a strong and significant increase ($P < 0.001$) with increased irradiance, where the violaxanthin de-epoxidation state increased throughout the day in both *Z. muelleri* ssp. *capricorni* and *H. ovalis* (Fig. 1e and f). On both days, the greatest violaxanthin de-

epoxidation occurred during air exposure (black arrows) in both species (Fig. 1e and f, respectively).

Initial effective quantum yield of PSII (Yi) from the RLC declined significantly ($P < 0.001$) with increased irradiance from 10:30 to 14:00 in *Zostera muelleri* ssp. *capricorni* with a further significant decline occurring during air exposure (Table 1A). The same pattern was seen in *Halophila ovalis* with a consistent decline in Yi with increasing *in situ* irradiance; however, only a significant drop ($P < 0.001$) in Yi occurred during exposure (Table 1B). The maximum rETR ($rETR_{max}$) and minimum saturating irradiance (E_k) values showed a light-dependent response in both species (Table 1 A and B), with a significant increase in $rETR_{max}$ with increased irradiance followed by a significant decline upon air exposure in both *Z. muelleri* ssp. *capricorni* ($P < 0.001$; Table 1A) and *H. ovalis* ($P = 0.011$; Table 1B). E_K was significantly greater at the maximum daily irradiance for both *Z. muelleri* ssp. *capricorni* ($P = 0.001$) and *H. ovalis* ($P = 0.003$; Table 1A and B). These changes in photosynthetic parameters further support the idea of additional stress to the plants when exposed, where seagrass, able to maintain high rates of electron transport at higher irradiance levelsonly seem to be able to do this if they are submerged (Table 1). Light utilisation efficiency (α) decreased throughout the day in *Z. muelleri* ssp. *capricorni*, declining with increased irradiance and dropped significantly as the plants became air-exposed ($P <0.001$; Table 1A). A similar pattern was seen in *H. ovalis* ($P = 0.001$; Table 1B), where increased irradiance lead to a decline in α. However, unlike *Z. muelleri* ssp. *capricorni*, there was no difference in α from the highest irradiance to being exposed, suggesting that the plant's ability to efficiently utilise the light available is not greatly impacted by air-exposed conditions and that in *H. ovalis* this parameter is more sensitive to high irradiance than air exposed conditions.

278 *Summer (growing season)*

279 *In situ* PAR varied throughout the day due to intermittent cloud cover. However, it was
280 maximal during tidal minimum on the 19th of January, with plants being air-exposed during
281 irradiances above 1600 μmol photons m^{-2} s^{-1} (Fig. 2a; Table 2A). On the 20th, PAR reached a
282 maximum one hour prior to exposure, but remained above 1000 μmol photons m^{-2} s^{-1} during
283 the exposure event (Fig. 2b; Table 2B). Oxygen production in *Zostera muelleri* ssp.
284 *capricorni* increased significantly with increasing irradiance as the tide withdrew (Fig. 2c).
285 Gross O_2 evolution just prior to air exposure was 2-3 times greater than the noon values
286 measured at ~ 1 m depth. The reduced light level at the end of the day may have contributed
287 to the decline in photosynthesis after re-immersion for *Z. muelleri* ssp. *capricorni* following
288 air exposure (Fig 2c). For *Halophila ovalis,* gross O_2 production rates didn't vary throughout
289 the tidal cycle. There was however, a significant decline in respiration rate at 14:00 (Fig d).
290 Seagrass photosynthetic light absorption capacity remained largely constant throughout the
291 tidal exposure event (0.48 ± 0.04, 0.46 ± 0.09, respectively). There was a significant increase
292 ($P < 0.001$) in the violaxanthin de-epoxidation state with increased irradiance (Fig. 2e and f).
293 In *Z. muelleri* ssp. *capricorni* the greatest violaxanthin de-epoxidation occurred during air
294 exposure (black arrows). A similar response was measured in *H. ovalis*; however, the last
295 time point did not drop following air exposure (Fig. 2f).

296 There was a significant decline ($P < 0.005$) in initial effective quantum yield of PSII (Yi)
297 during air exposure in *Zostera muelleri* ssp. *capricorni* and *Halophila ovalis* (Table 2).
298 Maximum rETR ($rETR_{max}$) and minimum saturating irradiance (E_k) values showed a light-
299 dependent response in both species (Table 2), although with some inconsistencies for *Z.*
300 *muelleri* ssp. *capricorni* (Table 2A). These were likely due to the intermittent cloud cover
301 during sampling which may have affected some of the fluorescence and PAR values. In both

species there was a significant decline in $rETR_{max}$ during air exposure ($P < 0.001$; Table 2). In both cases, irradiance was equally high immediately prior to and during air exposure, further supporting the suggestion of additional stress to the plants when exposed to desiccation, even when irradiance is optimal for greater rates of electron transport. Light utilisation efficiency (α) decreased throughout the day in both *Z. muelleri* ssp. *capricorni* and *H. ovalis*, declining with increased irradiance and then declining further as the plants became air-exposed ($P < 0.001$; Table 2). The significant recovery in α following exposure (Table 2A) emphasises the negative impact that air exposure has on the photosynthetic efficiency of *Z. muelleri* ssp. *capricorni*.

Autumn (senescent season)

The low tide (13:00 h) coincided with the maximum solar irradiance during the Autumn study, with PAR reaching in excess of 1800 μmol photons m^{-2} s^{-1} during air exposure (Fig. 3a and b). Consistent with the previous tidal exposure studies, rates of gross O_2 production in both species were significantly greater ($P < 0.01$) at 12:30 (just prior to air exposure) than at 10:10 and 14:10 (Fig. 3c and d). No change in dark respiration rate was found throughout the day in either species. During this collection trip, *Zostera muelleri* ssp. *capricorni* and *Halophila ovalis* were sampled on the same day and therefore incubated simultaneously, thus being exposed to identical light and temperature conditions. Interestingly, O_2 production rate appears more responsive to irradiance variations and air exposure in *Z. muelleri* ssp. *capricorni* than *H. ovalis* (Fig 3c and d, respectively), closely matching the chl *a* fluorescence data. In line with previous measurements, the fraction of light absorbed by seagrass leaves remained constant throughout the tidal cycle (0.46 ± 0.01, 0.49 ± 0.03, respectively), thus further confirming that these seagrass do not regulate their light capturing efficiency under rapidly changing light intensities. Also consistent with the previous two seasons, the

violaxanthin de-epoxidation state showed a significant increase in de-epoxidation ratio with increased irradiance ($P < 0.001$) and maximum de-epoxidation occurring during air exposure (Fig. 3e and f).

Initial effective quantum yield of PSII (Yi) showed a significant decline ($P < 0.001$) during air exposure and greatest irradiance in both species (Table 3), but with a greater decline measured for *Zostera muelleri* ssp. *capricorni*. A similar pattern was observed for maximum $rETR_{max}$ and α in *Z. muelleri* ssp. *capricorni* declining significantly during air exposure ($P = 0.012$ and $P = 0.001$; Table 3A), but recovering by 14:10. *Halophila ovalis* did not show the same trend in photosynthetic parameters (Table 3B). Instead, significant differences were only detected for $rETR_{max}$ at the lowest irradiance levels and deepest depth (8:30), where $rETR_{max}$ was greatest ($P < 0.047$) and during moderate light at 10:10 where $rETR_{max}$ dropped significantly ($P = 0.038$; Table 3B). Thus, it would seem that there was no clear response in $rETR_{max}$ to air exposure or irradiance in autumn for *H. ovalis* (Table 3B). No differences were detected in E_k or α between sampling times for *H. ovalis* also indicating no light-dependent response or sensitivity to desiccation.

Winter (senescent season)

Due to poor weather conditions, only one day of sampling was possible for this season. Therefore, data was only collected for *Zostera muelleri* ssp. *capricorni* for the winter period. Tidal and PAR data showed an inverse pattern, consistent with previous seasons, of high irradiance during low tide (Fig. 4a). Unlike previous seasons however, oxygen production declined significantly ($P < 0.05$) just before air exposure and then stayed low following exposure (Fig. 4b). This would suggest that the decline in photosynthesis was due to high irradiance and not necessarily air exposure, as was seen in the previous three seasons.

Seagrass photosynthetic light absorption capacity remained constant throughout the tidal exposure event (0.45 ± 0.01). Consistent with the other seasons, violaxanthin de-epoxidation state showed a significant increase in de-epoxidation ratio with increased irradiance ($P < 0.001$) with maximum de-epoxidation occurring during air exposure (Fig. 4c). Photosynthetic parameters Yi, $rETR_{max}$ and α all declined significantly ($P < 0.05$) during air exposure (Table 4), but did not differ during the other parts of the day and there was no significant change in E_k throughout the day.

*Light-dependent or air-exposed response***?**

To help differentiate a light-dependent response from the effects of air exposure, effective quantum yield of PSII (Yi) as a function of *in situ* irradiance was plotted for *Zostera muelleri* ssp. *capricorni* and *Halophila ovalis* (Fig. 5). Regression analyses were then performed on the data to ascertain the effect of air exposure on Yi. First, a regression analysis using all the Yi data was performed to elucidate the effect of light on Yi (Fig. 5a & c). Then another regression using only the Yi values obtained while seagrass were submerged (ie: in the absence of air-exposed data) was conducted to see if this altered the light-dependent response (Fig 5b & d). Yi for *Z. muelleri* ssp. *capricorni* showed a significant although weak negative correlation with increased irradiance ($R^2 = 0.3268$; $P < 0.0001$; Fig. 5a) when regression was applied to all the data (including the air-exposed data; Fig 5a). However, when only the submerged data were used (Fig. 5b), no correlation was detected ($R^2 = 0.0001$). In contrast, a significant relationship was detected in *H. ovalis* between Yi and irradiance under both air-exposed ($R^2 = 0.4872$; $P < 0.0001$; Fig. 5c) and submerged conditions ($R^2 = 0.3313$; $P < 0.0001$; Fig. 5d).

Discussion

All organisms growing in an intertidal habitat must tolerate oscillations in environmental conditions, some of which may act synergistically or antagonistically. Consequently, trying to ascertain the effect of a single environmental stressor is difficult in isolation of other environmental factors (Lee et al. 2007). For this reason, this study was focused on determining whether there was a significant change in photosynthesis over a tidal cycle, with particular interest to see how photosynthesis was impacted by low tide exposure and not on what was the main driver of this change. Several significant differences in physiological responses were detectable in both seagrass species and between seasons. The data show that oxygen evolution increased as the tide receded and then declined significantly immediately after air exposure during the growing season. This compliments the chl *a* fluorescence data, which further shows that during exposure, photosynthetic activity (Yi, rETRmax) declined as a result of increased photoinhibitory stress (increased de-epoxidation of violaxanthin). The increase in photosynthetic activity with increased irradiance in spring and summer (growing season) is consistent with previous studies that have found photoinhibition to be primarily absent in intertidal seagrasses (Beer and Björk 2000). The cause of the photosynthetic stress measured in this study during air exposure is still unknown; it could be the result of desiccation or excess heat or a combination of both. What is clear is air exposure during a tidal cycle did not provide these intertidal seagrass meadows with a 'window' of opportunity in which to maximise productivity.

The significant and seasonally consistent decline in photosynthetic efficiency (Yi) during air exposure for *Zostera muelleri* ssp. *capricorni* highlights the sensitivity of this intertidal species to exposed conditions. Light had very little effect on photosynthetic activity until it was combined with the negative effect of air exposure, in all seasons. *Z. muelleri* ssp.

399 *capricorni* has been shown to have a preference for higher irradiances, with significant
400 declines in carbon production and above ground biomass when grown in light levels that are
401 below saturating irradiances (Collier et al. 2011). This has major implications with respect to
402 daily productivity, as during low tide, when irradiance is maximal, photosynthetic activity
403 declines in response to exposure stress and not high irradiance, thus limiting the 'window' for
404 high rates of productivity to times of high irradiance with submergence. Although this
405 response was also seen in *Halophila ovalis*, it was only observed when it corresponded with
406 high irradiances and was rarely significantly different from the high irradiance response.
407 Indeed, in this study *H. ovalis* showed a stronger response to light condition than to exposure.
408 This absence of any correlation between effective quantum yield of PSII and air exposure for
409 *H. ovalis* could be a result of its morphology. The leaf stems are fine and unable to support
410 the leaves when the tide recedes, resulting in the leaves lying flat against the substrate and
411 often submerged in small pools of water, potentially providing protection against air exposure
412 (Björk et al. 1999).

413 For each season, measurements were taken close to midday low tide "windows" when light
414 levels were greatest. Cayabyab and Enriquez (2007) found a strong light-dependent response
415 in oxygen evolution rates in *Thalassia testudinum* with very similar values to those found in
416 this study (ranging from 0.5-2.0 μmol O_2 cm^{-2} h^{-1} over 50-2000 μmol photons m^{-2} s^{-1}). The
417 increase in photosynthetic activity with increased irradiance in the spring and summer studies
418 (growing season) would suggest that these species have a higher-light requirement for growth
419 and photosynthesis than what is normally available during high tide. It also suggests that they
420 take advantage of increased irradiances as the tide recedes. However, during autumn and
421 winter (senescent season) this type of opportunistic response by seagrasses is no longer
422 apparent (Lee et al. 2007). The fact that photosynthetic light absorption capacity (a*)
423 remained largely constant throughout the tidal exposure events across all seasons, as well as

the lack of change in leaf chlorophyll concentrations, confirms that these seagrass species do not regulate light capturing efficiency under rapidly changing irradiance. Furthermore, an a* of approx. 0.5 is consistent with the average values published by Campbell et al. (2007) for intertidal *H. ovalis* (0.52 ± 0.10) and *Z. capricorni* (0.60 ± 0.04) sampled along the northern Queensland coast.

Comparison of the data between seasons shows the greatest response to air-exposure for *Zostera muelleri* ssp. *capricorni* in the spring sampling month – ie a reduced response to exposure in late summer and the senescent seasons. This difference in stress during air exposure between the seasons could correspond to temperature differences or monthly light supply, both of which might play a significant role in the loss of photosynthetic efficiency in *Z. muelleri* ssp. *capricorni*. Water temperatures were more than five degrees warmer during the growing season (23.7-27.3ºC) compared with the senescent season (18.2-21.5ºC). Indeed, a recent study on *Z. muelleri* ssp. *capricorni* showed significant decline in photosynthesis, growth and carbon production at temperatures exceeding 31°C (Collier et al. 2011). The clear difference between spring and the other seasons is likely to be the result of a number of factors, rather than temperature alone. Average monthly irradiance varied from relatively high in spring (12.3 mol photons $m^{-2}d^{-1}$) to around of that half in summer (6.5 mol photons $m^{-2}d^{-1}$) and autumn (5.7 mol photons $m^{-2}d^{-1}$), before increasing again in winter (14.2 mol photons $m^{-2}d^{-1}$). This would suggest a potential synergistic effect between light and temperature, where spring showed combined high light and warmer temperature conditions. A similar result was found by Collier et al (2011) whereby high light in the presence of warmer temperatures led to reduced photosynthesis after 30 days, whereas high irradiance in the absence of high temperature showed no change in leaf photosynthesis. This provides a possible explanation for the difference in stress response measured between the spring and

summer (growing season) in this study. However, determination of the exact causality of these differences is beyond the scope of this study.

Similarly, the measured decline in effective quantum yield of PSII in response to high midday irradiances indicates that energy is being diverted from photochemistry to non-photochemical processes; this potentially results in substantial losses (up to 10%) in carbon assimilation (Long et al. 1994). Again this could relate to the warmer temperatures during the growing season (October and January), which showed higher respiration rates, potentially inhibiting carbon production (Balthuis 1983; Ralph 1998). These seasonal differences in physiological stress responses measured in this study (increased respiration rates and decline in effective quantum yield) would again suggest that temperature might play a key role in the loss in productivity during air exposure. One study found that in the absence of desiccation, high temperatures had minimal effect on seagrass health and physiology, but when exposed to high temperatures during air exposure, there was a significant decline in seagrass photosynthetic health (Seddon and Cheshire 2001).

Zostera muelleri ssp. *capricorni* and *Halophila ovalis* showed maximum de-epoxidation ratios during the growing season (maximum approx. 0.6) declining in the senescent season (maximum approx. 0.35). These maximum de-epoxidation ratios are within the same range (0.4 – 0.7) of those measured previously in *Zostera marina* (Ralph et al. 2002). The photoprotective pigment response measured over each tidal cycle, where de-epoxidation ratio increased with increased irradiance, was to be expected. However, the additional increase in de-epoxidation ratio during exposure provides further support for increased physiological stress under air exposed conditions. In several instances, this response occurred irrespective of irradiance being less during the exposure period than at other times in the day. Violaxanthin de-epoxidation ratio is an indicator of non-photochemical quenching, a

photoprotective response in which carotenoid pigments are utilised to dissipate excess photon energy as heat (Demmig-Adams & Adams, 1996). The light-dependent increase in de-epoxidation ratio indicates increased heat dissipation from the light harvesting antenna of PSII. However, when combined with the significant decline in photosynthetic efficiency (Yi), this data provides strong evidence that under air-exposed conditions, less photon energy is being utilised for photochemistry and a larger proportion is being lost as heat, thus, providing protection for the cell when electron transport and photosynthesis are compromised by the external environmental conditions.

The results from this study have successfully demonstrated that tidal exposure does not provide intertidal seagrass meadows with a 'window' of respite from high turbidity. Furthermore, this study has increased our understanding of *in situ* photosynthetic efficiency and measured changes in oxygen evolution and physiology as a result of changes in irradiance and water depth over a tidal cycle. The seasonal variability in the response of these two species to air exposure has provided a greater understanding of annual patterns in seagrass photosynthetic activity under natural tidal fluctuations and has demonstrated the need for seagrass to have access to high light in turbid coastal environments during the early growing season when compared with the senescent season. This has important management implications when considering the impact of coastal development, such as dredging operations, in estuaries and harbours.

Acknowledgements

The authors would like to thank Dr Vinod Kumar and Marlene Zbinden for their assistance and support on this project. This project was funded by Gladstone Ports Corporation Limited and the Queensland Department of Agriculture Fisheries and Forestry and Australian Research Council grant (LP110200454) awarded to PJR and MR.

496

497 **References**

498 Abal E, Dennison W (1996) Seagrass depth range and water quality in southern Moreton
499 Bay, Queensland, Australia. Mar and Freshwater Res 47:763-771

500 Beer S, Björk M (2000) Measuring rates of photosynthesis of two tropical seagrasses by
501 pulse amplitude modulated (PAM) fluorometry. Aquat Bot 66:69-76

502 Beer S, Rehnberg J (1997) The acquisition of inorganic carbon by the seagrass Zostera
503 marina. Aquat Bot 56:277-283

504 Bulthuis DA (1983) Effects of temperature on the photosynthesisirradiance curve of the
505 Australian seagrass, *Heterozostera tasmanica*. Mar Biol Lett 4: 47-57

506 Björk M, Uku J, Weil A, Beer S (1999) Photosynthetic tolerances to desiccation of tropical
507 intertidal seagrasses. Mar Ecol Prog Ser 191:121-126

508 Cabello-Pasini A, Lara-Turrent C, Zimmerman RC (2002) Effect of storms on
509 photosynthesis, carbohydrate content and survival of eelgrass populations from a
510 coastal lgoon and the adjacent open ocean. Aquat Bot 74: 149-164

511 Campbell S, McKenzie L, Kerville S, Bite J (2007) Patterns in tropical seagrass
512 photosynthesis in relation to light, depth and habitat. Estuar Coast Shelf Sci 73:551-
513 562

514 Cayabyab N, Enriquez S (2007) Leaf photoacclimatory responses of the tropical seagrass
515 *Thalassia testudinum* under mesocosm conditions: a mechanistic scaling-up study.
516 New Phytologist 176:108-123

517 Collier CJ, Uthicke S, Waycott M (2011) Thermal tolerance of two seagrass species at
518 contrasting light levels: Implications for future distribution in the Great Barrier Reef.
519 Limnol and Oceanogr 56:000-000
520 Demmig-Adams B, Adams WW (1996) Xanthophyll cycle and light stress in nature: uniform
521 response to excess direct sunlight among higher plant species. Planta 198:460-470
522 Dennison WC, Orth RJ, Moore KA, Stevenson JC, Cater V, Kollar S, Bergstrom PW, Batiuk
523 A (1993) Assessing water quality with submerged aquatic vegetation. BioScience 43:
524 86-94
525 Duarte CM (1991) Seagrass depth limited. Aquat Bot 40: 363-377
526 Durako MJ (2007) Leaf optical properties and photosynthetic leaf absorptances in several
527 Australian seagrasses. Aquat Bot 87:83-89
528 Enriquez S (2005) Light absorption efficiency and the package effect in the leaves of the
529 seagrass *Thalassia testudinum.* Mar Ecol Prog Ser 289:141-150
530 Jeffrey SW, Humphrey GF (1975) New spectrophotometric equations for determining
531 chlorophyll *a, b, c1,* and *c2* in higher plants and natural phytoplankton. Biochem
532 Physiol Pfl 165:191-94
533 Johnston AM, Raven JA (1986) The analysis of photosynthesis in air and water of
534 *Ascophyllum nodosum* L. Jol. Oecologia 69:288-295
535 Lee K-S, Dunton KH (1997) Effects of in sity light reduction on the maintenance, growth and
536 partitioning of carbon resources in Thalassia testudinum Banks ex König. J Exp Mar
537 Biol Ecol 210: 53-73
538 Lee K-S, Park SR, Kim YK (2007) Effects of irradiance, temperature, and nutrients on
539 growth dynamics of seagrasses: A review. J Exp Mar Biol Ecol 350:144-175
540 Leuschner C, Landwehr S, Mehlig U (1998) Limitation of carbon assimilation of intertidal
541 Zostera noltii and Z. marina by desiccation at low tide. Aquat Bot 62:171-176

Long SP, Humphries S, Falkowski PG (1994) Photoinhibition of Photosynthesis in Nature. Annu Rev Plant Physiol Plant Mol Biol 45:633-662

Longstaff B, Dennison W (1999) Seagrass survival during pulsed turbidity events: the effects of light deprication on the seagrasses *Halodule pinifolia* and *Halophila ovalis*. Aquat Bot 65:105-121

Nabe H, Funabiki R, Kashino Y, Koike H, Satoh K (2007) Responses to Desiccation Stress in Bryophytes and an Important Role of Dithiothreitol-Insensitive Non-Photochemical Quenching Against Photoinhibition in Dehydrated States. Plant Cell Physiol 48:1548–1557

Olesen B, Enríquez S, Duarte CM, Sand-Jensen K (2002) Depth-acclimation of photosynthesis, morphology and demography of Posidonia oceanica and Cymodocea nodosa in the Spanish Mediterranean Sea. Mar Ecol Prog Ser 236: 89-97

Orth RJ, Carruthers TJB, Dennison WC, Duarte CM, Fourqurean JW, Heck Jr KL, Hughes AR, Olyarnik S, Williams SL, Kendrick GA, Kenworthy WJ, Short FT, Waycott M (2006) A Global Crisis for Seagrass Ecosystems. BioScience 56:987-996

Ralph P, Polk S, Moore K, Orth R, Smith Jr W (2002) Operation of the xanthophyll cycle in the seagrass *Zostera marina* in response to variable irradiance. J Exp Mar Biol Ecol 271:189-207

Ralph PJ (1998) Photosynthetic response of laboratory-cultured Halophila ovalis to thermal stress. Mar Ecol Prog Ser 171:123-130

Ralph PJ, Gademann R (2005) Rapid light curves: A powerful tool to assess photosynthetic activity. Aquat Bot 82:222-237

Ralph PJ, Durako MJ, Enríquez S, Collier CJ and Doblin MA (2007) Impact of light limitation on seagrasses. J Exp Mar Biol Ecol 350:176-193

566 Rasheed, M.A. and Unsworth, R.K.F. (2011) Long-term climate-associated dynamics of a
567 tropical seagrass meadow: implications for the future. Marine Ecology Progress
568 Series Vol. 422 93-103.
569 Rasheed, M.A., Dew, K.R., McKenzie, L.J., Coles, R.G., Kerville, S.P. and Campbell, S.J.
570 (2008) Productivity, carbon assimilation and intra-annual change in tropical reef
571 platform seagrass communities of the Torres Strait, north-eastern Australia.
572 Continental Shelf Research Vol 28, 2292-2304.
573 Seddon S, Cheshire AC (2001) Photosynthetic response of Amphibolis antarctica and
574 Posidonia australis to temperature and desiccation using chlorophyll fluorescence.
575 Mar Ecol Prog Ser 220:119-130
576 Taylor, H.A. and Rasheed, M.A. (2011) Impacts of a fuel oil spill on seagrass meadows in a
577 subtropical port, Gladstone, Australia – The value of long-term marine habitat
578 monitoring in high risk areas. Marine Pollution Bulletin 63: 431-437
579 Thayer SS, Björkman O (1990) Leaf Xanthophyll content and composition in sun and shade
580 determined by HPLC. Photosynth Res 23:331-343
581 Unsworth RKF, Cullen LC (2010) Recognising the necessity for Indo-Pacific seagrass
582 conservation. Conservation Lett 3:63-73
583 van Heukelem L, Thomas C (2001) Computer-assisted high-performance liquid
584 chromatography method development with applications to the isolation and analysis
585 of phytoplankton pigments. J Chromatogr A 910:31-49
586 Zimmerman RC, Reguzzoni JL, Wyllie-Echeverria S, Josselyn M, Alberte RS (1991)
587 Assessment of environmental suitability for growth of Zostera marina L. (eelgrass) in
588 San Francisco Bay. Aquat Bot 39:353-366

589

Tables:

Table 1: Photosynthetic parameters initial effective quantum yield of photosystem II (Yi), maximum electron transport rate ($rETR_{max}$), minimum saturating irradiance (E_k) and light utilisation efficiency (α) calculated from the rapid light curves of A) *Zostera muelleri* ssp.

609 *capricorni* and B) *Halophila ovalis* (24th October, 2010). PAR (µE) = µmol photons m^{-2} s^{-1}.
610 Data represent means ± SD (n = 6). Superscript letters indicate significant differences at $\alpha <$
611 0.05.

A. *Zostera muelleri* ssp. *capricorni* SPRING				
Time	10:30	12:00	14:00	15:40
PAR (µE)	240-320	358-510	792-774	733-543
Water depth (m)	1.9	1.5	0.2	Exposed
Yi	0.726 ± 0.010^{a}	0.702 ± 0.020^{a}	0.647 ± 0.026^{b}	0.598 ± 0.036^{c}
$rETR_{max}$	69.90 ± 4.800^{ab}	84.04 ± 7.330^{bc}	84.90 ± 12.20^{c}	55.05 ± 11.90^{a}
E_k	70.90 ± 5.400^{a}	97.70 ± 9.020^{bc}	108.3 ± 27.40^{b}	79.90 ± 7.880^{c}
α	0.980 ± 0.020^{a}	0.860 ± 0.020^{b}	0.820 ± 0.110^{b}	0.680 ± 0.130^{c}
B. *Halophila ovalis*				
Time	10:30	12:00	14:00	15:40
PAR (µE)	240-320	358-510	792-774	733-543
Water depth (m)	1.9	1.5	0.2	Exposed
Yi	0.737 ± 0.020^{a}	0.673 ± 0.014^{a}	0.657 ± 0.081^{a}	0.549 ± 0.102^{b}
$rETR_{max}$	69.60 ± 13.20^{a}	74.80 ± 12.75^{ab}	91.10 ± 16.80^{b}	64.10 ± 7.500^{a}
E_k	69.00 ± 15.40^{a}	79.40 ± 18.60^{a}	113.0 ± 21.50^{bc}	84.50 ± 15.60^{ac}
α	1.000 ± 0.040^{a}	0.960 ± 0.090^{a}	0.810 ± 0.028^{b}	0.770 ± 0.080^{b}

612
613
614
615
616
617
618
619

620 Table 2: Photosynthetic parameters initial effective quantum yield of photosystem II (Yi),
621 maximum electron transport rate ($rETR_{max}$), minimum saturating irradiance (E_k) and light
622 utilisation efficiency (α) calculated from the rapid light curves of A) *Zostera muelleri* ssp.

capricorni (19th January, 2011) and B) *Halophila ovalis* (20th January, 2011) Data represent means ± SD (n = 6). Superscript letters indicate significant differences at $\alpha < 0.05$.

A. *Zostera muelleri* ssp. *capricorni* SUMMER					
Time	11:00	12:00	13:30	15:00	16:30
PAR (μE)	400	86	1550	1692	320
Water depth (m)	2.5	1.0	0.3	Exposed	0.2
Yi	0.773 ± 0.010[a]	0.737 ± 0.042[a]	0.730 ± 0.030[a]	0.346 ± 0.081[b]	0.607 ± 0.080[a]
$rETR_{max}$	40.27 ± 3.160[a]	28.62 ± 5.300[b]	37.48 ± 3.510[a]	10.65 ± 3.030[c]	37.41 ± 7.750[ab]
E_k	99.49 ± 8.360[a]	74.06 ± 12.39[b]	102.7 ± 9.130[a]	60.52 ± 13.58[b]	130.8 ± 23.82[c]
α	0.410 ± 0.010[a]	0.380 ± 0.030[a]	0.360 ± 0.030[a]	0.170 ± 0.030[b]	0.280 ± 0.040[c]
B. *Halophila ovalis*					
Time	11:30	12:30	13:45	15:00	16:00
PAR (μE)	153	741	591	1200	1053
Water depth (m)	2.0	1.0	0.6	0.05	Exposed
Yi	0.759 ± 0.022[a]	0.741 ± 0.018[a]	0.734 ± 0.017[a]	0.614 ± 0.076[a]	0.436 ± 0.053[b]
$rETR_{max}$	15.64 ± 2.590[a]	26.82 ± 4.960[ab]	28.17 ± 8.170[b]	42.20 ± 13.95[b]	14.74 ± 5.910[ca]
E_k	36.70 ± 6.190[a]	61.86 ± 13.52[b]	69.22 ± 23.03[b]	145.1 ± 46.89[c]	69.34 ± 31.91[ab]
α	0.430 ± 0.060[a]	0.440 ± 0.020[a]	0.410 ± 0.030[a]	0.310 ± 0.030[b]	0.220 ± 0.030[c]

Table 3: Photosynthetic parameters initial effective quantum yield of photosystem II (Yi), maximum electron transport rate ($rETR_{max}$), minimum saturating irradiance (E_k) and light utilisation efficiency (α) calculated from the rapid light curves of *Zostera muelleri* ssp. *capricorni* and *Halophila ovalis* (14th May 2011). Data represent means ± SD (n = 6 *Z.*

637 *muelleri* ssp. *capricorni*; *n* = 4, *H. ovalis*). Superscript letters indicate significant differences

638 at $\alpha < 0.05$.

A. *Zostera muelleri* ssp. *capricorni* AUTUMN				
Time	08:30	10:10	13:00	14:10
PAR (µE)	350	750	1800	750
Water depth (m)	1.5	0.5	Exposed	0.5
Yi	0.749 ± 0.019[a]	0.732 ± 0.034[a]	0.535 ± 0.070[b]	0.719 ± 0.050[a]
$rETR_{max}$	71.84 ± 15.23[a]	67.79 ± 21.24[a]	37.69 ± 9.798[b]	67.74 ± 22.23[a]
E_k	78.79 ± 18.61[a]	73.04 ±	58.63 ± 17.16[a]	83.23 ± 26.48[a]
α	0.916 ± 0.041[a]	25.86[a]0.937 ± 0.040[a]	0.674 ± 0.194[b]	0.812 ± 0.067[a]
B. *Halophila ovalis*				
Time	08:30	10:10	13:00	14:10
PAR (µE)	350	750	1800	750
Water depth (m)	1.5	0.5	Exposed	0.5
Yi	0.723 ± 0.022[a]	0.638 ± 0.100[ab]	0.609 ± 0.072[b]	0.733 ± 0.033[a]
$rETR_{max}$	82.24 ± 21.30[a]	40.82 ± 15.54[b]	51.92 ± 15.21[b]	53.15 ± 21.90[b]
E_k	86.61 ± 23.21[a]	44.41 ± 15.13[a]	60.56 ± 24.51[a]	54.04 ± 22.75[a]
α	0.954 ± 0.062[a]	0.921 ± 0.619[a]	0.888 ± 0.112[a]	0.978 ± 0.114[a]

639

640

641

642

643

644

645

646

647 Table 4: Photosynthetic parameters initial effective quantum yield of photosystem II (Yi),

648 maximum electron transport rate ($rETR_{max}$), minimum saturating irradiance (E_k) and light

649 utilisation efficiency (α) calculated from the light response curves of *Zostera muelleri* ssp.

650 *capricorni* (14th July, 2011). Data represent means ± SD (*n* = 6). Superscript letters indicate

651 significant differences at $\alpha < 0.05$.

Zostera muelleri ssp. *capricorni* WINTER				
Time	10:00	11:30	13:15	15:35
PAR (μE)	400	800	1800	350
Water depth (m)	1.8	1.0	Exposed	0.4
Yi	0.736 ± 0.017^{a}	0.712 ± 0.023^{a}	0.558 ± 0.049^{b}	0.694 ± 0.036^{a}
$rETR_{max}$	92.77 ± 45.17^{a}	105.6 ± 27.56^{a}	57.40 ± 12.39^{b}	92.64 ± 23.72^{a}
E_k	101.3 ± 57.37^{a}	121.0 ± 41.12^{a}	75.15 ± 18.77^{a}	107.3 ± 30.89^{a}
α	0.939 ± 0.086^{a}	0.894 ± 0.082^{a}	0.776 ± 0.095^{b}	0.871 ± 0.055^{ab}

652

653

654

655

656

657

658

659

660

661

662

663

664 Figure captions:

665 Figure 1: Photosynthetically active radiation (PAR) at the depth of the seagrass and water

666 depth over the spring tidal cycles on the 23rd and 24th of October 2010 (a and b, respectively),

667 gross oxygenic photosynthesis (black bars) and dark respiration (grey bars) *in situ* for the
668 intertidal seagrass species (c) *Zostera muelleri* ssp. *capricorni* and (d) *Halophila ovalis*.
669 Violaxanthin de-epoxidation ratio for (e) *Z. muelleri* ssp. *capricorni* and (f) *H. ovalis* during
670 tidal cycles on the 22nd and 24th of October 2010, respectively. Data represent mean ± SEM
671 (n = 6), superscript letters indicate significant differences at $\alpha < 0.05$ and down arrows
672 indicate time of air exposure at low tide.

673

674 Figure 2: Photosynthetically active radiation (PAR) at the depth of the seagrass and water
675 depth over summer tidal cycles on the 19th and 20th of January 2011 (a and b, respectively),
676 gross oxygenic photosynthesis (black bars) and dark respiration (grey bars) *in situ* for the
677 intertidal seagrass species (c) *Zostera muelleri* ssp. *capricorni* and (d) *Halophila ovalis*.
678 Violaxanthin de-epoxidation ratio for (e) *Z. muelleri* ssp. *capricorni* and (f) *H. ovalis*. Data
679 represent mean ± SEM (n = 6), superscript letters indicate significant differences at $\alpha < 0.05$
680 and down arrows indicate time of air exposure at low tide.

681

682 Figure 3: Photosynthetically active radiation (PAR) at the depth of the seagrass and water
683 depth over an autumn tidal cycle on the 14th of May 2011 (a and b), gross oxygenic
684 photosynthesis (black bars) and dark respiration (grey bars) *in situ* for the intertidal seagrass
685 species (c) *Zostera muelleri* ssp. *capricorni* and (d) *Halophila ovalis*. Violaxanthin de-
686 epoxidation ratio for *Z. muelleri* ssp. *capricorni* (e) and *H. ovalis* (f) during a tidal cycle. Data
687 represent mean ± SEM (*Z. muelleri* ssp. *capricorni* n = 6; *H. ovalis* n = 4), superscript letters
688 indicate significant differences at $\alpha < 0.05$ and down arrows indicate time of air exposure at
689 low tide.

690

691 Figure 4: Photosynthetically active radiation (PAR) at the depth of the seagrass and water
692 depth over a winter tidal cycle on the 14th of July 2011 (a), gross oxygenic photosynthesis
693 (black bars) and dark respiration (grey bars) *in situ* for the intertidal seagrass species *Zostera*
694 *muelleri* ssp. *capricorni* (b). Violaxanthin de-epoxidation ratio for *Z. muelleri* ssp. *capricorni*
695 (c) during a tidal cycle. Data represent mean ± SEM (n = 6), superscript letters indicate
696 significant differences at $\alpha < 0.05$ and down arrows indicate time of air exposure at low tide.

697

698 Figure 5: Initial effective quantum yield (Yi) as a function of *in situ* irradiance (PAR µmol
699 photons m^{-2} s^{-1}) in (a & b) *Zostera muelleri* ssp. *capricorni* and (c & d) *Halophila ovalis* for
700 all data (submerged and air-exposed) collected during tidal cycle (a & c) and yield obtained
701 during submersion only (b & d). Dots represent all data collected from each field study (all
702 four seasons). The relationships between Yi and irradiance were fitted using linear regression
703 (solid line) and the R^2 values are provided in the legend.

704

705

706

707

708

709 Figures:

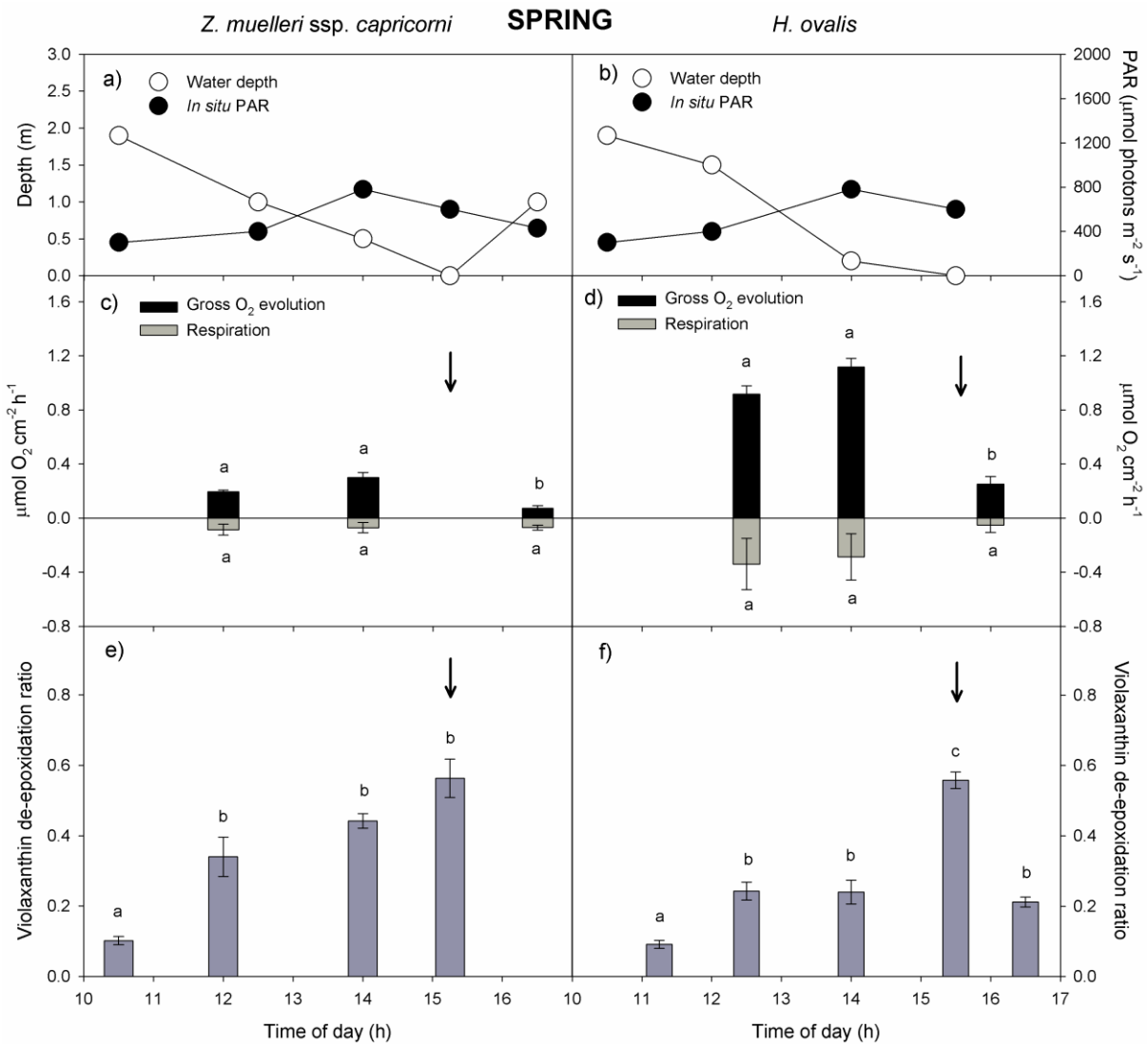
Z. muelleri ssp. capricorni
SPRING
H. ovalis
a)
Water depth
In situ PAR
b)
Water depth
In situ PAR
Depth (m)
PAR (µmol photons m-2 s-1)
c)
Gross O2 evolution
Respiration
d)
Gross O2 evolution
Respiration
µmol O2 cm-2 h-1
e)
f)
Violaxanthin de-epoxidation ratio
Time of day (h)
Time of day (h)

Figure 1

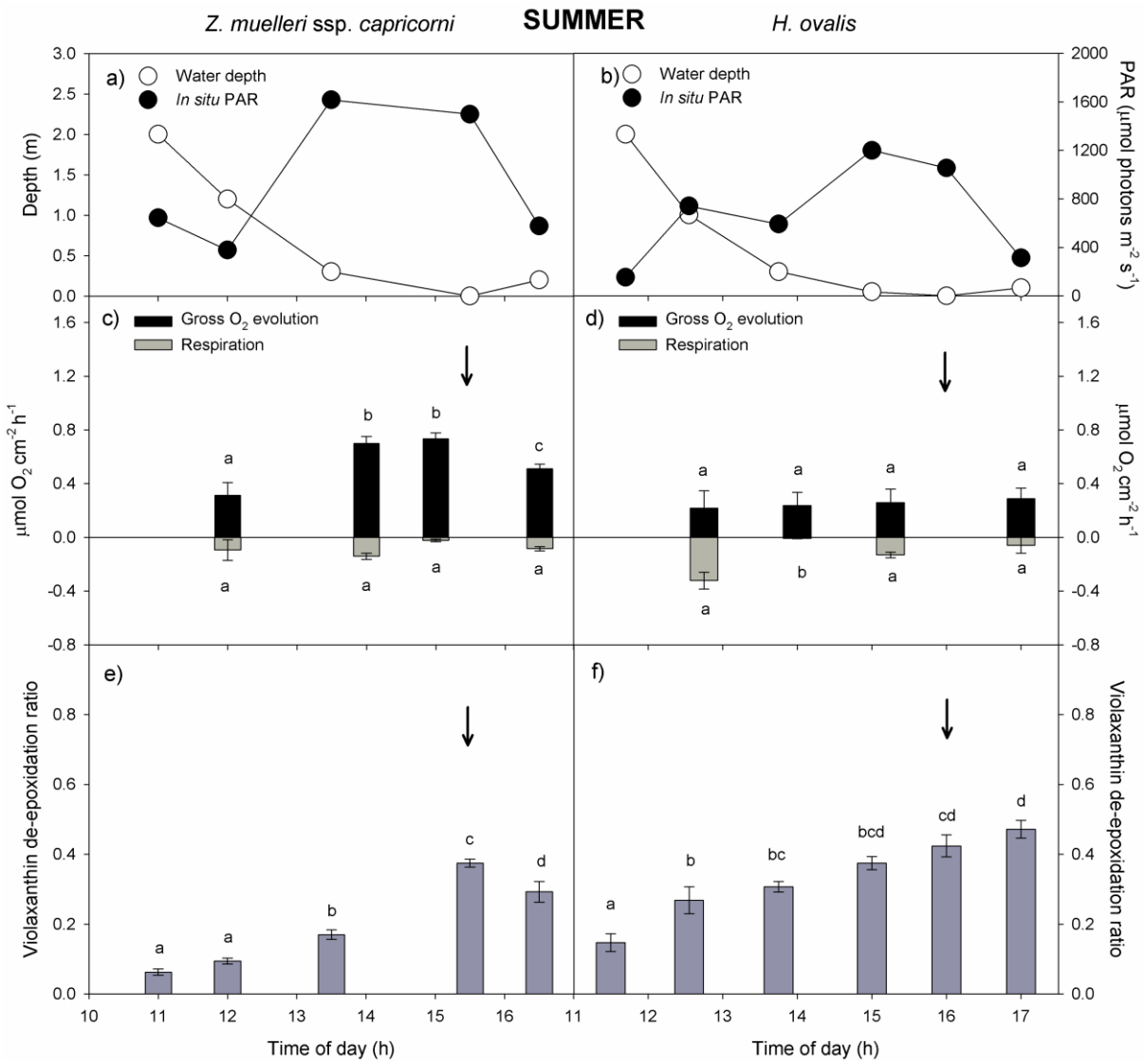
Z. muelleri ssp. capricorni
SUMMER
H. ovalis
a)
Water depth
In situ PAR
b)
Water depth
In situ PAR
Depth (m)
PAR (µmol photons m-2 s-1)
c)
Gross O2 evolution
Respiration
d)
Gross O2 evolution
Respiration
µmol O2 cm-2 h-1
e)
f)
Violaxanthin de-epoxidation ratio
Time of day (h)
Time of day (h)

Figure 2

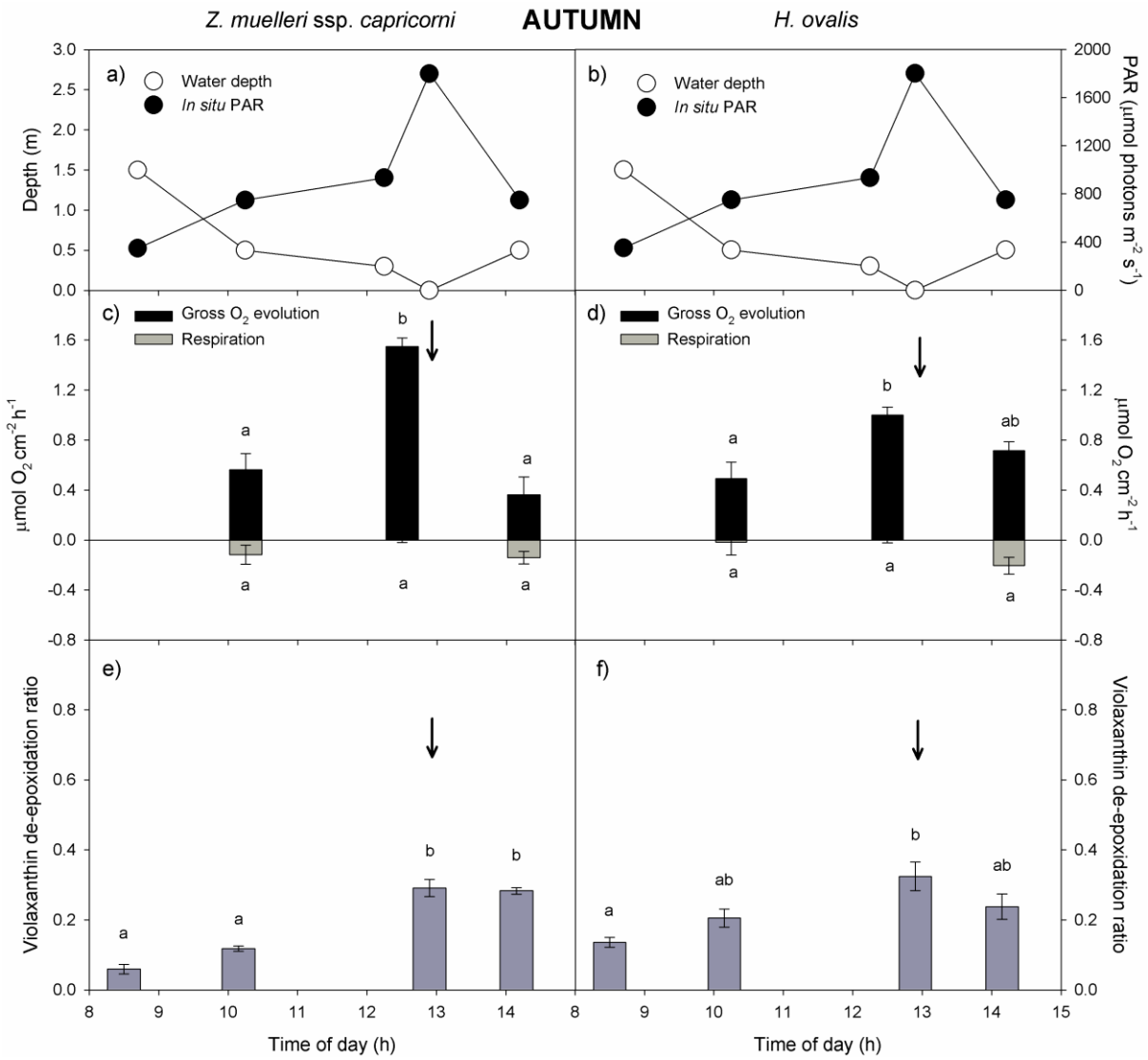
Z. muelleri ssp. capricorni
AUTUMN
H. ovalis
a)
b)
c)
d)
e)
f)
Water depth
In situ PAR
Depth (m)
PAR (µmol photons m-2 s-1)
Gross O2 evolution
Respiration
µmol O2 cm-2 h-1
Violaxanthin de-epoxidation ratio
Time of day (h)

Figure 3

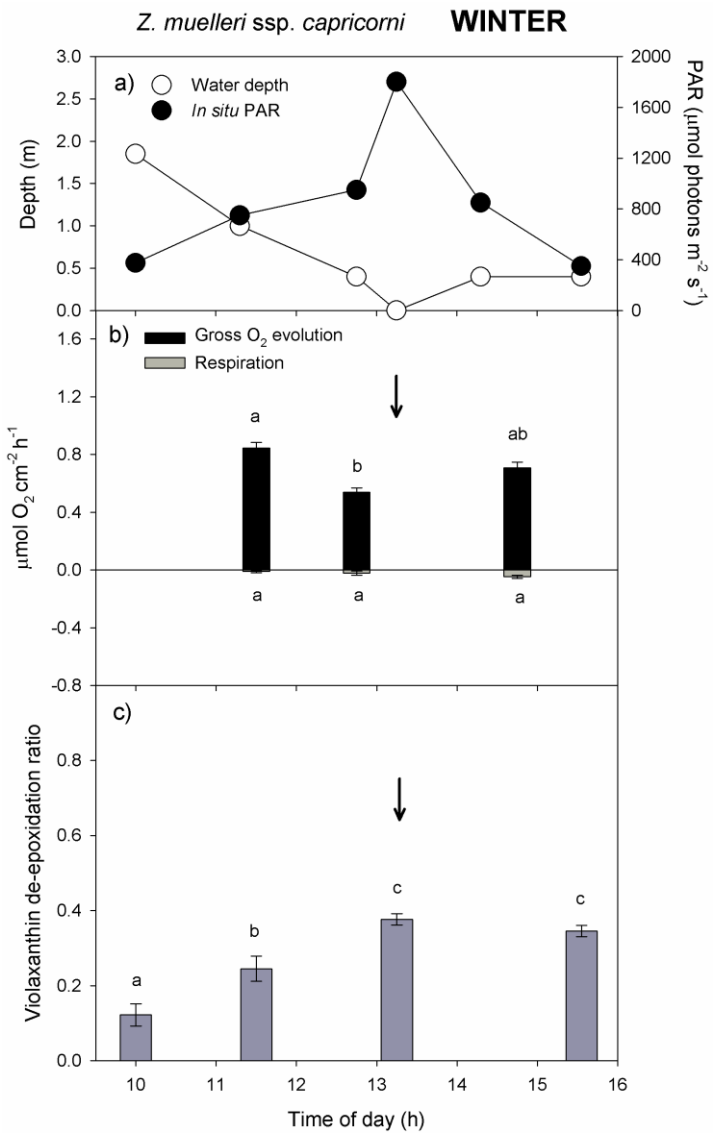

731

732

733

734

735

736 Figure 4

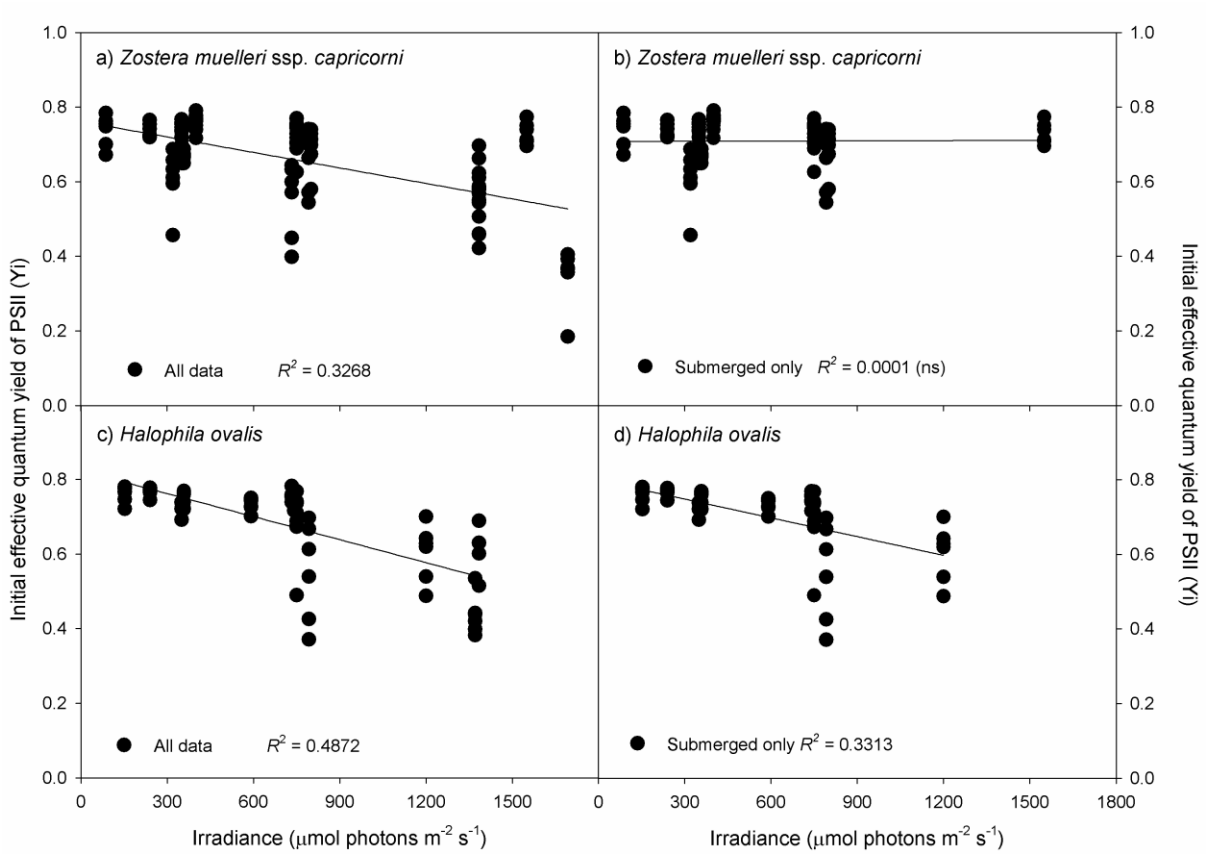

737

738

739

740

741

742

743 Figure 5

744